ELSEVIER

Materials Science and Engineering A 481–482 (2008) 462–465

MATERIALS SCIENCE & ENGINEERING A

www.elsevier.com/locate/msea

Ni_4Ti_3 precipitate structures in Ni-rich NiTi shape memory alloys

D. Holec [a,b], O. Bojda [a,c], A. Dlouhý [a,*]

[a] *Academy of Sciences CR, Institute of Physics of Materials, Žižkova 22, 616 62 Brno, Czech Republic*
[b] *University of Cambridge, Dep. of Materials Science & Metallurgy, Pembroke Street, Cambridge CB2 3QZ, UK*
[c] *Brno University of Technology, Faculty of Chemistry, Purkyňova 118, 612 00 Brno, Czech Republic*

Received 26 October 2006; accepted 2 November 2006

Abstract

Non-uniform distributions of Ni_4Ti_3 precipitate crystallographic variants are investigated in a Ni-rich NiTi shape memory alloy after aging, assisted by external stress. A finite-element method model is presented that considers the elastic anisotropy of the B2 parent phase and also mutual misorientations of grains in a polycrystalline sample. On loading by the external stress, the stress is redistributed in the microstructure and the precipitation of some Ni_4Ti_3 crystallographic variants becomes distinctly favorable in grain boundary regions since these variant configurations minimize the elastic interaction energy. The volume fraction of the affected grain boundary regions is calculated and the numerical results are compared with the data obtained by differential scanning calorimetry and transmission electron microscopy.

Keywords: NiTi shape memory alloys; Ni_4Ti_3 precipitates; Heat treatment; Multi-step martensitic transformations

1. Introduction

Processing routes of Ni-rich NiTi shape memory alloys (SMAs) are often completed by standardization annealing and subsequent aging where metastable coherent Ni_4Ti_3 particles precipitate [1,2]. The particles have a rhombohedral structure (space group *R*3), a lenticular shape and belong to one of eight crystallographic variants that grow on $\{1\,1\,1\}$-planes of the B2 NiTi matrix [3,4]. These precipitates give rise to coherency stress fields [4,5] and the external stress applied during aging can favor the occurrence of certain precipitate crystallographic variants [6–9]. At the same time, the precipitation of Ni-rich Ni_4Ti_3 particles changes the Ni-content in the surrounding NiTi matrix [10,11]. Both, the coherency stresses and the variations in the local Ni-concentration influence transitions from the cubic B2 austenite to the monoclinic B19′ martensite. The presence of Ni_4Ti_3 particles not only supports the occurrence of R-phase in the range of intermediate temperatures between the B2 and B19′ regimes [12,13], but also results in a more complicated path of the $R \rightarrow$ B19′ transition [4,8,10,14–17]. It is generally accepted that these martensitic transformations (MTs) govern the NiTi shape memory behavior [1].

Heat treatments performed without the assistance of external stress in combination with a specific Ni-content of the alloy result in a heterogeneous precipitation of the Ni_4Ti_3 phase [8,18]. In these cases particles nucleate and grow only in regions close to grain boundaries in NiTi polycrystals while grain interiors remain particle free. The heterogeneous precipitation causes a splitting of $R \rightarrow$ B19′ transition into two transformation steps [8,14,17]. A similar $R \rightarrow$ B19′ transformation path was observed for the particle structures formed during aging assisted by the external stress [8]. In these microstructures, the number density of Ni_4Ti_3 particles was homogeneous but the distribution of Ni_4Ti_3 crystallographic variants was heterogeneous [9]. In their recent paper, Fan et al. introduced a term the large-scale heterogeneity for these non-uniformities in the Ni_4Ti_3 particle population [17]. On the other hand, the local stress state and Ni-concentration variations in the vicinity of individual particles may also result in a complicated MT path [4,10,19] and these effects have been classified as the small-scale heterogeneity [17]. In order to account quantitatively for the influence of various Ni_4Ti_3 particle structures on the characteristics of MTs, it is essential to (i) understand how these microstructures form and (ii) obtain reliable quantitative data on particle sizes and distributions. The present study focuses on the distribution of Ni_4Ti_3 particle variants after the aging assisted by the external stress. Using a numerical simulation, we demonstrate that the heterogeneous distribution of particle variants may be rationalized

* Corresponding author. Tel.: +420 532 290 412; fax: +420 541 218 657.
E-mail address: dlouhy@ipm.cz (A. Dlouhý).

0921-5093/$ – see front matter © 2007 Elsevier B.V. All rights reserved.
doi:10.1016/j.msea.2006.11.182

by a redistribution of the external stress in the polycrystalline microstructure due to the B2-lattice anisotropy.

2. Deconvolution of the DSC signal

The transformation heat h released or absorbed during MTs in the Ti–50.7 at.% Ni alloy after annealing (1123 K/900 s/water) and after annealing followed by the stress-assisted aging (773 K/3.6 ks/8 MPa or 20 MPa) was recorded in differential scanning calorimetry (DSC) experiments and presented in our earlier work [8,9]. In the present study, we use the same DSC data and we focus on the $R \rightarrow B19'$ transition on cooling. As it is illustrated in Fig. 1, this transition exhibits a two-step character after the stress-assisted aging, the two steps being represented by two DSC peaks M1 and M2. With increasing level of the applied stress, the portion of the transformation heat associated with the M1 peak increases. A transmission electron microscopy (TEM) study [9] indicated that the individual transformation steps M1 and M2 might be related to different martensite growth conditions in the grain boundary regions (M1 peak) and in the grain interior (M2 peak). It has been found that these two regions differ in the distribution of individual Ni_4Ti_3 particle variants (the large-scale heterogeneity of the type II [9,17]). According to this scenario, the amount of heat associated with the transformation step M1 should be proportional to the volume fraction of grain boundary regions affected by the heterogeneous Ni_4Ti_3 variant distribution. Since the transformation heat is also proportional to the area under the DSC curve, a deconvolution of the DSC signal can yield quantitative data on the volume fraction in question. As a result of this analysis, the volume fraction data obtained from the DSC experiments can be compared to the results of the TEM study [9].

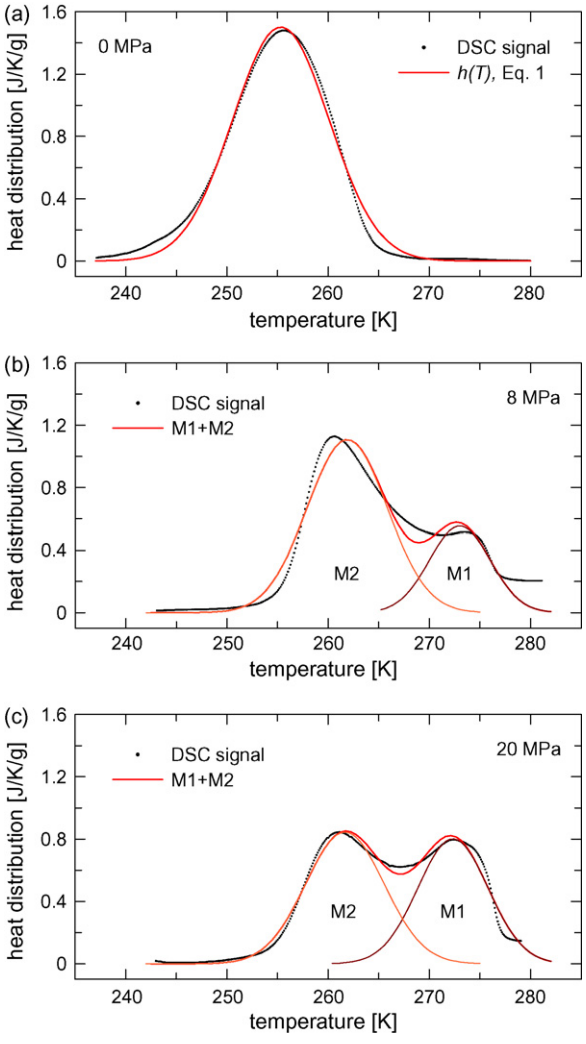

Fig. 1. DSC charts of MTs in the Ti–50.7 at% Ni alloy: (a) the transition $B2 \rightarrow B19'$ after annealing (1123 K/900 s/water), (b) the transition $R \rightarrow B19'$ after annealing followed by stress-assisted aging (773 K/3.6 ks/8 MPa) and (c) the transition $R \rightarrow B19'$ after annealing followed by stress-assisted aging (773 K/3.6 ks/20 MPa). The DSC signal in (b) and (c) is decomposed into individual peaks M1 and M2.

Three DSC charts in Fig. 1 were recorded after annealing (Fig. 1a) and annealing followed by the stress-assisted aging (Fig. 1b and c). Experimental values are plotted using individual data points and the continuous curves represent distribution functions that were fitted to the experimental data in order to deconvolute the composed M1 + M2 peak. First, a function

$$h(T) = h_{T_p} e^{-1/2((T-T_p)/\Delta)^2} \quad (1)$$

is fitted to the single DSC peak in Fig. 1a (the $B2 \rightarrow B19'$ transition). As it follows from Fig. 1a, the normal distribution characterized by the parameters $h_{T_p} = 1.5\,J\,K^{-1}\,g^{-1}$, $T_p = 255.3$ K and $\Delta = 4.75$ K satisfactorily describes the partition of the transformation heat h with temperature T. Therefore, the similar type of distribution was used to separate the individual M1 and M2 peaks that make up the $R \rightarrow B19'$ transition after the stress-assisted aging. Results of the deconvolution are presented in Fig. 1b and c, where individual normal distributions represent the peaks M1 and M2 and their sum approximates the composed M1 + M2 peak. Finally, the areas delimited by the individual peaks M1 and M2 and by the composed peak M1 + M2 were evaluated. Table 1a and b summarizes the results for stresses 8 and 20 MPa, respectively.

3. Applied stress redistribution and precipitation of Ni_4Ti_3 variants

Recent experimental TEM studies confirmed that the application of the uniaxial external stress during aging results in a

Table 1
Characteristics of DSC heat signal shown in Fig. 1 and measured after aging at 773 K/1 h assisted by external stresses: (a) 8 and (b) 20 MPa [8,9]

Peak	h_{T_p} [J K^{-1} g^{-1}]	T_p [K]	Δ [K]	Peak area [J g^{-1}]
(a)				
M1	0.56	273.2	3.00	4.2
M2	1.11	261.9	3.96	11.0
M1 + M2	–	–	–	15.2
(b)				
M1	0.80	272.5	3.47	7.0
M2	0.84	262.0	3.88	8.2
M1 + M2	–	–	–	15.2